Brain Tumor Segmentation in Fluid-Attenuated Inversion Recovery Brain MRI using Residual Network Deep Learning Architectures

Mohamed Mahyoub
Tutor Reach
United Kingdom
m.mahyoub@tutorreach.com

Friska Natalia
Faculty of Engineering and Informatics
Universitas Multimedia Nusantara
Tangerang, Indonesia
friska.natalia@umn.ac.id

Sud Sudirman
School of Computer Science and
Mathematics
Liverpool John Moores University
Liverpool, United Kingdom
s.sudirman@ljmu.ac.uk

Abdulmajeed Hammadi Jasim Al-Jumaily
Universiti Putra Malaysia
Serdang, Malaysia
a.aljumaily@ieee.org

Panos Liatsis
Khalifa University
Abu Dhabi, United Arab Emirates
panos.liatsis@ku.ac.ae

Abstract—**Early and accurate detection of brain tumors is very important to save the patient's life. Brain tumors are generally diagnosed manually by a radiologist by analyzing the patient's brain MRI scans which is a time-consuming process. This led to our study of this research area for finding out a solution to automate the diagnosis to increase its speed and accuracy. In this study, we investigate the use of Residual Network deep learning architecture to diagnose and segment brain tumors. We proposed a two-step method involving a tumor detection stage, using ResNet50 architecture, and a tumor area segmentation stage using ResU-Net architecture. We adopt transfer learning on pre-trained models to help get the best performance out of the approach, as well as data augmentation to lessen the effect of data population imbalance and hyperparameter optimization to get the best set of training parameter values. Using a publicly available dataset as a testbed we show that our approach achieves 84.3% performance outperforming the state-of-the-art using U-Net by 2% using the Dice Coefficient metric.**

Keywords—Brain Tumor; Image Segmentation; Magnetic Resonance Imaging; Residual Networks; Deep Learning

I. INTRODUCTION

Fluid attenuated inversion recovery (FLAIR) is an MRI sequence that uses a special inversion recovery sequence with a long inversion time. This technique removes the signal from the cerebrospinal fluid (CSF) that makes brain tissue appear similar to that in T2-weighted sequence images but with grey matter brighter than white matter, and the CSF is dark instead of bright. The usefulness of FLAIR sequences in identifying many diseases of the central nervous system has been reported in the literature. This includes the detection of multiple sclerosis lesions [1], subarachnoid hemorrhage [2], and head injuries [3]. More importantly, FLAIR imaging has also been shown to be a valuable imaging modality in the assessment of intra-axial brain tumors [4].

Some types of brain tumors are very aggressive. They are reported to be the biggest killer of children and adults under 40 years old. Brain tumors account for between 85% and 90% of all primary central nervous system tumors. It is estimated that around 308,102 people worldwide were diagnosed with a primary brain tumor or spinal cord tumor in 2020 alone [5].

Although they are more common in older adults, brain tumors have also been seen in children as well. Around 88,000 children and adults are estimated to be living with a brain tumor in the UK currently [6].

The effectiveness of the treatment mainly depends on the accuracy of the diagnosis. Brain tumors are usually diagnosed through biopsies and brain scans. They can also be diagnosed through a neurological exam, which is a variety of neurological tests that examine neurological functions. It consists of several questions to check the patient's mental status and find out any abnormalities related to hearing, vision, senses, balance, reflexes, etc. Biopsies are the least safe way to perform a diagnosis since it involves tissue collection from the affected area. If the procedure is possible, doctors would be able to identify the grade of the tumor very accurately, which is the most important factor in determining the best line of treatment. Lastly, brain tumors can be diagnosed using imaging technologies. Several imaging technologies such as Computed Tomography (CT) scan, Positron Emission Tomography (PET) scan, and Magnetic Resonance Imaging (MRI), are commonly used in the diagnosis process, with the latter believed to be the most popular [7].

There are more than 150 different types of brain tumors with three different ways of classifying them. The first classification is based on the origin of the tumors, whether they originate from the tissue of the brain (primary brain tumors) or from elsewhere in the body (metastatic brain tumors). The second classification is based on whether the tumor started from glial or non-glial cells. And lastly, brain tumors can be classified as either benign or malignant.

The detection of brain tumor areas in the brain is performed through segmentation and is based on its size, shape, position, and boundaries. The process is performed manually by an expert radiologist. The speed and accuracy of the manual segmentation process depend on the level of expertise of the radiologist. In this paper, we detail the result of our investigation into using a deep learning approach to perform automatic segmentation of brain tumor regions in brain MRI. We use brain FLAIR MRI scans from a publicly available dataset. This should allow other researchers to reproduce our results to confirm our findings.

II. Literature Review

There are various popular deep learning architectures used by the computer vision community, including convolutional neural networks (CNNs), recurrent neural networks (RNNs), long-short term memory (LSTM), encoder-decoders, and generative adversarial networks (GANs). With the rise in popularity of deep learning, various other deep neural architectures, such as transformers, capsule networks, gated recurrent units, spatial transformer networks, etc., have also been developed. The use of CNNs has been proposed extensively in the healthcare domain. A few examples are; early detection of fetal heart diseases [8], measurements of organ sizes [9], semantic segmentation of organs [10][11] or cancerous tissues [12], and finding the causes of disease [13].

In the domain of brain tumor detection and segmentation, the deep learning approach is very popular. Raut et al. [14] automate the detection of brain tumors using CNN and the segmentation of tumor areas using K-mean and autoencoders. The study reported an accuracy of 95.6% on testing data with an F1 score of 96%. Ezhilarasi and Varalakshmi proposed a system that marks the tumor area and defines the type of brain tumor using the AlexNet model along with Region Proposal Network derived using the Faster R-CNN algorithm [15]. The use of Faster R-CNN is mainly to detect the tumor object in an MRI image and create a bounding box on the tumor with its class along with the score.

Luo et al. [16] used lightweight HDC-Net, a hierarchical decoupled convolution network for brain tumor segmentation. The paper concludes that, despite the promising performance in terms of the time taken by the model to run, it could not reach the expected accuracy. Another study by Rahimpour et al. [17] is based on multiple combinations of multi-sequence MRI datasets. They evaluated early fusion and late fusion CNN models based on DeepMedic architecture [18] for the segmentation task. The feature maps are concatenated in low-level feature space for the early fusion strategy; thus, the network can only evaluate a basic link between multiple MRI sequences. The late fusion strategy, on the other hand, integrates the feature maps extracted for each type of sequence in the high-level layer, allowing it to better use the distinctive information of each type of sequence. While both techniques perform similarly in terms of segmentation, the late fusion strategy is more versatile and offers greater flexibility in terms of incorporating all available MRI data.

While many papers reported the superiority of deep learning approaches when compared to machine learning classifiers, there have also been some works using the hybrid approach where both methods are combined to get the best out of it. One such study was done by Cui et al. where the authors [19] proposed a two-stage process. In the first stage, a CNN model is trained to map the tumor label space. The predicted label by the CNN model then gets transferred to the SVM classifier where the segmentation task is done. The study observed that the performance of the hybrid model based on CNN and the SVM classifier performed better than the individual segmentation models based on CNN or SVM only.

In this study, we will also adopt a two-stage process similar to several methods proposed in the literature. The description of our methodology and the dataset used are given in the next section.

III. Material and Method

A. Dataset

The dataset used in this study contains 3929 brain MRI scans of 110 brain tumor patients suffering from lower-grade glioma. The image data is from The Cancer Genome Atlas - Low-Grade Glioma (TCGA-LGG) collection published by the Cancer Imaging Archive [20]. The data is taken from five institutions in the United States, 16 patients from the Thomas Jefferson University (TCGA-CS), 45 from the Henry Ford Hospital (TCGA-DU), one from the University of North Carolina (TCGA-EZ), 14 from the Case Western (TCGA-FG), and 34 from the Case Western – St. Joseph's (TCGA-HT). The assessment of tumor regions was based on fluid-attenuated inversion recovery (FLAIR) abnormality from which the manual segmentation masks are developed. This dataset is public [21] and has been used in several research works in the past [4].

The characteristics of the patients whose data is taken from and the characteristics of the tumor are shown in Tables I and II, respectively [4].

TABLE I. PATIENTS' CHARACTERISTICS

Characteristics	Value
Total Patients	110
Age (Median)	47
Age (Range)	20-75
Gender (Female)	56
Gender (Male)	53
Gender (Unknown)	1

TABLE II. TUMOR CHARACTERISTICS IN THE DATASET

Characteristics	Value
Grade II Astrocytoma	8
Grade III Astrocytoma	25
Grade II Oligoastrocytoma	14
Grade III Oligoastrocytoma	15
Grade II Oligodendroglioma	29
Grade III Oligodendroglioma	18
Not Available	1
IDH wild type (Glioblastomas)	25
IDH mutation with 1p/19q co-deletion	26
IDH mutation without 1p/19q co-deletion	56
Not Available	3

Although the data is taken from patients who have been confirmed to suffer from a brain tumor, not all of the 3929 images contain areas marked as a brain tumor, There are 1373 images has brain tumor regions and 2556 images that do not. An example image that has a brain tumor region is shown in Figure 1.
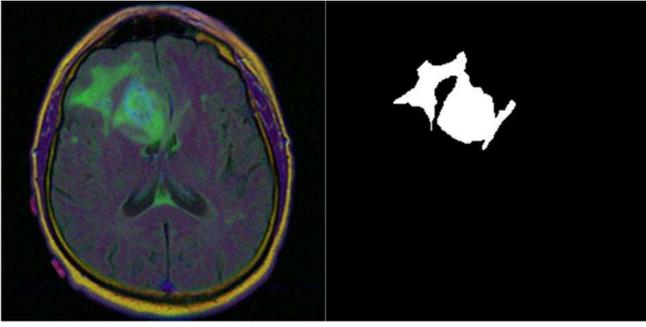
Fig. 1. An example image of a brain MRI FLAIR scan (left) with its associated mask marking the area of the glioma (right).

B. Methodology

The methodology we adopted in this study is illustrated in Figure 2. There is a two-step process that involves the tumor detection stage and tumor area segmentation stage.
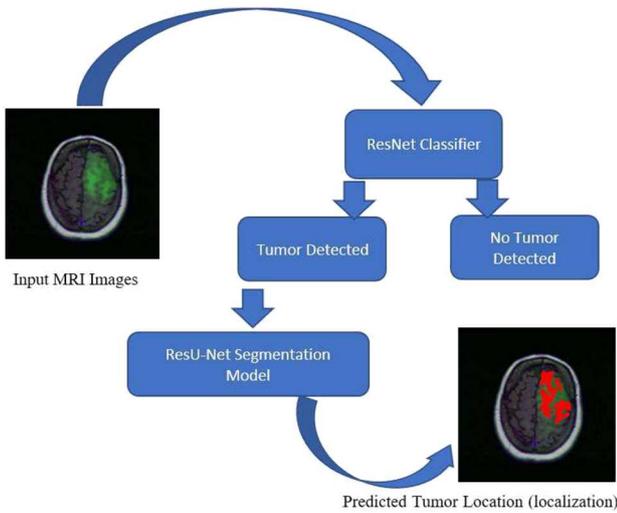

Fig. 2. A flowchart illustrating the two-step process adopted as the methodology. The first is to determine if the image contains a brain tumor using the ResNet50 classifier and the second is tumor region segmentation using ResU-Net.

ResNet50, one of the variants of the ResNet model [22] will be used in this study in the tumor detection stage. This architecture is 50-layer deep including 48 Convolution layers, one MaxPool layer, and one Average Pool layer. Overall, the model architecture is composed of five stages, each comprising an Identity block and a Convolution block, each having three Convolution layers. The three layers are 1×1, 3×3, and 1×1 convolutions. The reduction and subsequent restoration of the dimensions are accomplished using the 1×1 layers. The 3×3 layer is left as a bottleneck with smaller input/output dimensions. There are, in total, around 23 million trainable parameters in the ResNet50.

We will use a pre-trained model using the ImageNet database [23]. Transfer learning will be utilized in this model by replacing the final layers with a new classification layer of two outputs (either tumor or non-tumor image). The weights of the feature extraction layers are fixed during the training process.

We will use ResU-Net, or Residual U-Net, architecture for the tumor area segmentation stage. U-Net is a very popular and successful deep-learning network for semantic segmentation[24]. ResU-Net combines U-Net backbone architecture with residual blocks. This way it overcomes the problem of vanishing gradients which is observed in many deep-learning models. This customized U-Net architecture is based on fully convolutional networks. ResU-Net is very effective for image segmentation tasks that allow pixel-wise classification or localization.

Our method addresses the issue of data imbalance through data augmentation. This process artificially increases the amount of data by generating new data from existing data. Our data augmentation method applies some minor alterations to the original dataset to generate new images in the same latent space of the original data to amplify the dataset size. Our method also applies hyperparameter optimization when training the ResU-Net models to get the best possible models. We do not apply hyperparameter optimization when training the ResNet50 model since we manage to get a very good model with default parameter values.

IV. EXPERIMENT AND RESULT ANALYSIS

In our experiment, the dataset is split into three sets namely training, validation, and testing with a ratio of 70:15:15, respectively. The data augmentation is done with the parameters range shown in Table III.

TABLE III.   DATA AUGMENTATION PARAMETERS VALUES

	Value
Rotation Range	90
Width Shift Range	0.3
Heigh Shift Range	0.3
Shear Range	0.5
Zoom Range	0.3
Fill Mode	Reflect or Nearest
Horizontal Flip	True
Vertical Flip	True

As mentioned in the previous section, the ResNet50 model is trained using transfer learning and without hyperparameter optimization. This is because the classification performance of the model has met our target the first time. This is shown in Table IV.

TABLE IV.   CLASSIFICATION PERFORMANCE OF THE RESNET50 MODEL

	Precision	Recall	F1-Score	Support
0	0.97	1	0.98	362
1	1	0.95	0.97	214
Micro Average	0.98	0.98	0.98	576
Macro Average	0.98	0.97	0.98	576
Weighted Average	0.98	0.98	0.98	576

The ResU-Net model on the other hand is trained with hyperparameter optimization. The list of hyperparameters in which space is searched is shown in Table V. We repeat the training three times, one for a different number of maximum epochs which are 25, 60, and 150. The values of the hyperparameters of the final best models are shown in Table VI.

TABLE V.   HYPERPARAMETERS LIST

Hyperparameters	Value
Optimizers	SGDM/ADAM
Learning Rate	1e-04 – 5e-02
Kernel Initializer	Normal/Uniform
Dropout Rate	0.1/0.2/0.3
Epsilon	0.1/None
Batch Size	8/16/32

TABLE VI.   OPTIMIZED HYPERPARAMETERS VALUES FOR DIFFERENT EPOCH LENGTHS

Hyperparameters	Model A	Model B	Model C
Epochs	25	60	150
Optimizers	ADAM	ADAM	ADAM
Learning Rate	5e-02	1e-04	1e-04
Kernel Initializer	Normal	Uniform	Uniform
Dropout Rate	0.3	0.3	0.3
Epsilon	0.1	None	None
Batch Size	16	32	32

We show the training logs of the training process of the best model in each experiment in Figures 3, 4, and 5. These logs show that the training processes are relatively stable, and produce reasonable training and validation accuracies throughout the training period which indicates good generalization performance.

The segmentation performance of the three models is measured using Loss, Intersection over Union (IoU), and Dice Coefficients. The results are shown in Table VII. The table shows that the hyperparameter optimization process produces better models as we increase the number of epochs for training. The IoU metric appears to remain relatively high for all models. This suggests that it is the result of class population imbalance between tumor and non-tumor pixels, so we can argue that IoU is not a good metric to use. On the other hand, Dice Coefficient and Loss do manage to differentiate the performance of the models well.

TABLE VII.   MODEL PERFORMANCE ON TESTING SET

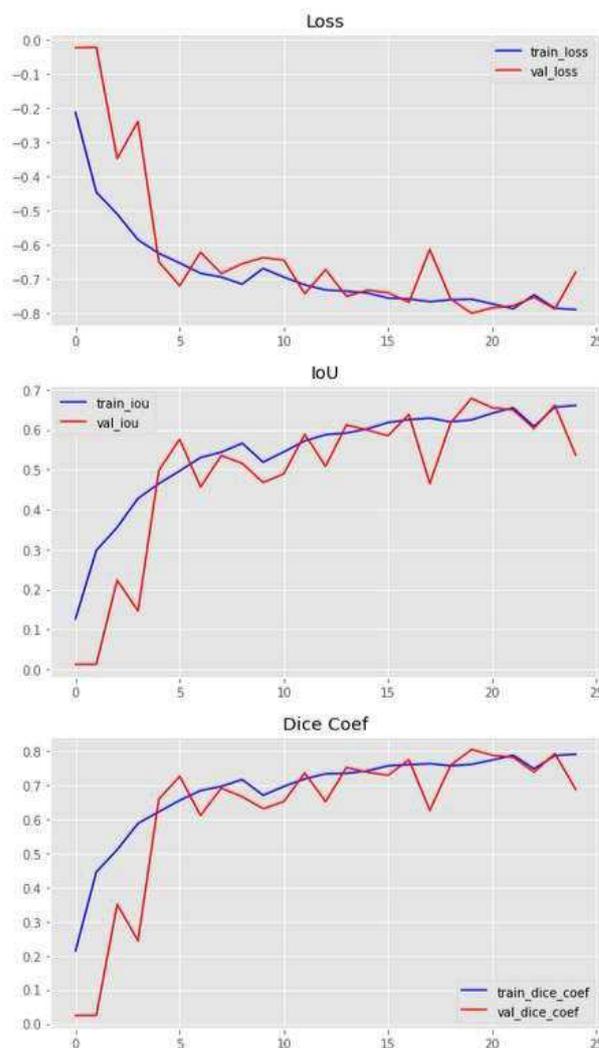| Optimized Model	No. of Epoch	Loss	IoU	Dice Coefficient
Model A	25	0.755	0.996	0.635
Model B	60	0.900	0.998	0.821
Model C	150	0.912	0.998	0.843

Fig. 3. Training log of the best ResU-Net model (Model A) after Hyperparameter optimization when max epoch is set to 25.

When compared to a similar experiment on the same dataset using U-Net [4], the result of our best model (Model C) using our method seems to perform better. The paper reported a mean Dice Coefficient of 82% compared to 84.3% in ours.
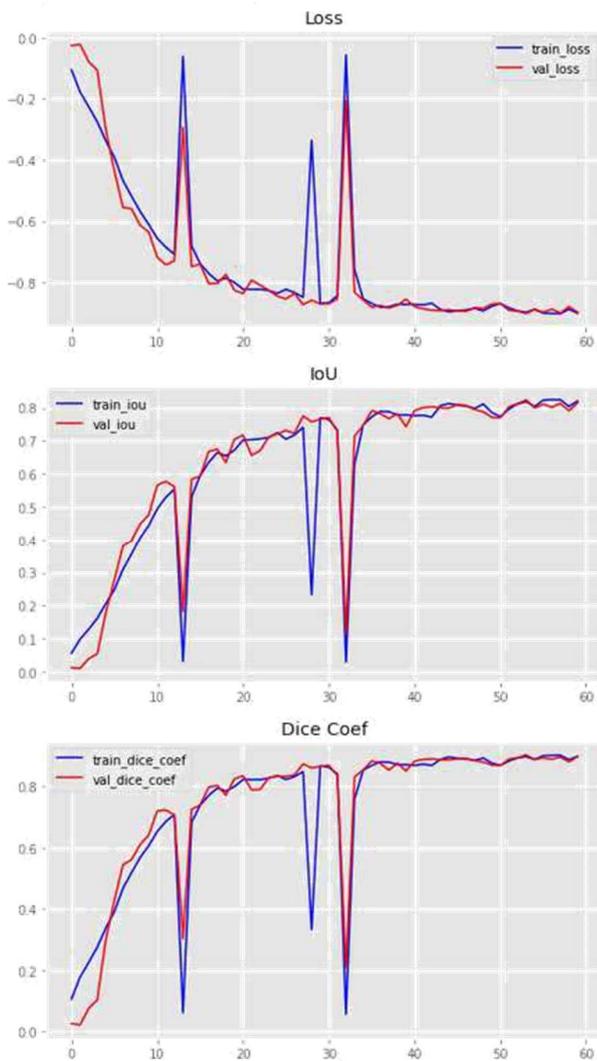
Fig. 4. Training log of the best ResU-Net model (Model B) after Hyperparameter optimization when max epoch is set to 60.
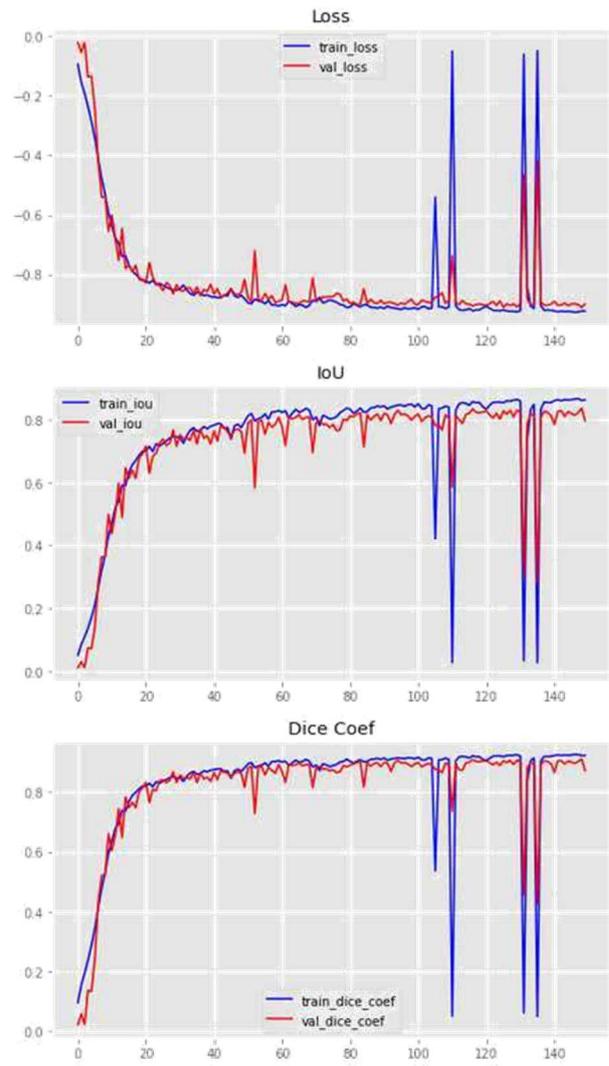

Fig. 5. Training log of the best ResU-Net model (Model C) after Hyperparameter optimization when max epoch is set to 150.

V. CONCLUSION

We have presented in this paper the results of our experiment of using deep learning approaches to perform brain tumor segmentation in MRI FLAIR images. Our two-step method involves a tumor detection stage and a tumor area segmentation stage performed in sequence. The tumor detection stage uses ResNet50 architecture whereas the tumor area segmentation stage uses ResU-Net architecture. We adopt transfer learning on pre-trained models to help get the best performance out of the approach, as well as data augmentation to lessen the effect of data population imbalance and hyperparameter optimization to get the best set of training parameter values. Our method is implemented on a publicly available dataset and we have shown that our best-developed model outperforms the state-of-the-art using the U-Net model reported in the literature.

REFERENCES

[1] R. Bakshi, S. Ariyaratana, R. H. B. Benedict, and L. Jacobs, "Fluid-attenuated inversion recovery magnetic resonance imaging detects cortical and juxtacortical multiple sclerosis lesions," *Arch. Neurol.*, vol. 58, no. 5, pp. 742–748, 2001.

[2] T. Okuda, Y. Korogi, I. Ikushima, R. Murakami, K. Nakashima, T. Yasunaga, Y. Kondo, and M. Takahashi, "Use of fluid-attenuated inversion recovery (FLAIR) pulse sequences in perinatal hypoxic-

ischaemic encephalopathy.," *Br. J. Radiol.*, vol. 71, no. 843, pp. 282–290, 1998.

[3] N. K. Bangerter, B. A. Hargreaves, G. E. Gold, D. T. Stucker, and D. G. Nishimura, "Fluid-attenuated inversion-recovery SSFP imaging," *J. Magn. Reson. Imaging An Off. J. Int. Soc. Magn. Reson. Med.*, vol. 24, no. 6, pp. 1426–1431, 2006.

[4] M. Buda, A. Saha, and M. A. Mazurowski, "Association of genomic subtypes of lower-grade gliomas with shape features automatically extracted by a deep learning algorithm," *Comput. Biol. Med.*, vol. 109, pp. 218–225, 2019.

[5] Cancer.Net Editorial Board, "Brain Tumor: Statistics," *Cancer.Net*, 2022. [Online]. Available: https://www.cancer.net/cancer-types/brain-tumor/statistics. [Accessed: 27-Oct-2022].

[6] The Brain Tumour Charity, "The statistics about brain tumours," *The Brain Tumour Charity*, 2022. [Online]. Available: https://www.thebraintumourcharity.org/get-involved/donate/why-choose-us/the-statistics-about-brain-tumours/. [Accessed: 27-Oct-2022].

[7] R. Sille, T. Choudhury, P. Chauhan, and D. Sharma, "A Systematic Approach for Deep Learning Based Brain Tumor Segmentation.," *Ingénierie des Systèmes d'Information*, vol. 26, no. 3, 2021.

[8] C. Song, T. Gao, Y. Gong, S. Sudirman, H. Wang, and H. Zhu, "Fully Automatic Ultrasound Fetal Heart Image Detection and Segmentation based on Texture Analysis," *Invest. Clin.*, vol. 61, no. 2, pp. 600–608, 2020.

[9] F. Natalia, H. Meidia, N. Afriliana, J. C. Young, R. E. Yunus, M. Al-Jumaily, A. Al-Kafri, and S. Sudirman, "Automated measurement of anteroposterior diameter and foraminal widths in MRI images for lumbar spinal stenosis diagnosis," *PLoS One*, vol. 15, no. 11, pp. 1–27, 2020.

[10] A. S. Al Kafri *et al.*, "Segmentation of lumbar spine MRI images for stenosis detection using patch-based pixel classification neural network," in *2018 IEEE Congress on Evolutionary Computation (CEC)*, 2018, pp. 1–8.

[11] A. S. Al-Kafri, S. Sudirman, A. Hussain, D. Al-Jumeily, F. Natalia, H. Meidia, N. Afriliana, W. Al-Rashdan, M. Bashtawi, and M. Al-Jumaily, "Boundary Delineation of MRI Images for Lumbar Spinal Stenosis Detection Through Semantic Segmentation Using Deep Neural Networks," *IEEE Access*, vol. 7, pp. 43487–43501, 2019.

[12] I. Despotović, B. Goossens, and W. Philips, "MRI segmentation of the human brain: challenges, methods, and applications," *Comput. Math. Methods Med.*, vol. 2015, 2015.

[13] A. S. Al-Kafri, S. Sudirman, A. Hussain, P. J. Fergus, D. Al-Jumeily, M. Al-Jumaily, and H. Al-Askar, "A Framework on a Computer Assisted and Systematic Methodology for Detection of Chronic Lower Back Pain Using Artificial Intelligence and Computer Graphics Technologies," in *Lecture Notes in Computer Science*, 2016, pp. 843–854.

[14] G. Raut, A. Raut, J. Bhagade, J. Bhagade, and S. Gavhane, "Deep Learning Approach for Brain Tumor Detection and Segmentation," in *2020 International Conference on Convergence to Digital World-Quo Vadis (ICCDW)*, 2020, pp. 1–5.

[15] R. Ezhilarasi and P. Varalakshmi, "Tumor detection in the brain using faster R-CNN," in *2018 2nd International Conference on I-SMAC (IoT in Social, Mobile, Analytics and Cloud)(I-SMAC) I-SMAC (IoT in Social, Mobile, Analytics and Cloud)(I-SMAC), 2018 2nd International Conference on*, 2018, pp. 388–392.

[16] Z. Luo, Z. Jia, Z. Yuan, and J. Peng, "HDC-Net: Hierarchical decoupled convolution network for brain tumor segmentation," *IEEE J. Biomed. Heal. Informatics*, vol. 25, no. 3, pp. 737–745, 2020.

[17] M. Rahimpour, K. Goffin, and M. Koole, "Convolutional neural networks for brain tumor segmentation using different sets of MRI sequences," in *2019 IEEE Nuclear Science Symposium and Medical Imaging Conference (NSS/MIC)*, 2019, pp. 1–3.

[18] K. Kamnitsas, E. Ferrante, S. Parisot, C. Ledig, A. V Nori, A. Criminisi, D. Rueckert, and B. Glocker, "DeepMedic for brain tumor segmentation," in *International workshop on Brainlesion: Glioma, multiple sclerosis, stroke and traumatic brain injuries*, 2016, pp. 138–149.

[19] B. Cui, M. Xie, and C. Wang, "A deep convolutional neural network learning transfer to SVM-based segmentation method for brain tumor," in *2019 IEEE 11th International Conference on Advanced Infocomm Technology (ICAIT)*, 2019, pp. 1–5.

[20] National Cancer Institute, "Cancer Imaging Archieve," *National Institutes of Health*, 2022. [Online]. Available: https://www.cancerimagingarchive.net/. [Accessed: 27-Oct-2022].

[21] M. Buda, "Brain MRI segmentation: Brain MRI images together with manual FLAIR abnormality segmentation masks," *Kaggle*, 2019. [Online]. Available: https://www.kaggle.com/datasets/mateuszbuda/lgg-mri-segmentation. [Accessed: 27-Oct-2022].

[22] K. He, X. Zhang, S. Ren, and J. Sun, "Deep residual learning for image recognition," in *Proceeding of IEEE Conference on Computer Vision and Pattern Recognition*, 2016, pp. 770–778.

[23] A. Krizhevsky, I. Sutskever, and G. E. Hinton, "Imagenet classification with deep convolutional neural networks," in *Advances in Neural Information Processing Systems*, 2012, pp. 1097–1105.

[24] O. Ronneberger, P. Fischer, and T. Brox, "U-net: Convolutional networks for biomedical image segmentation," in *Lecture Notes in Computer Science (including subseries Lecture Notes in Artificial Intelligence and Lecture Notes in Bioinformatics)*, 2015, vol. 9351.

[25] Z. Zhang, Q. Liu, and Y. Wang, "Road Extraction by Deep Residual U-Net," *IEEE Geosci. Remote Sens. Lett.*, vol. 15, no. 5, pp. 749–753, 2018.